Supplementary Figure Legends

Supplementary Figure S1. Targeted disruption of *Rassf2* animals and postnatal lethality in such mice. (**A**) Homologous recombination was confirmed by Southern blot analysis of genomic DNA from ES cells and mice with the 3′ external probe. The positions of hybridizing Eco*RI* fragments corresponding to wild-type (11.5 kb) and targeted (9 kb) *Rassf2* alleles are indicated (*left*). Genotyping PCR analysis and reverse transcription (RT)–PCR analysis of *Rassf2* mRNA in mouse embryonic fibroblasts for wild-type, *Rassf2*$^{+/-}$, and *Rassf2*$^{-/-}$ mice. The 887- and 392-bp products corresponding to the wild-type and mutant *Rassf2* alleles, respectively, are indicated (*right*). (**B**) Immunoblot analysis of wild-type (WT) and *Rassf2*$^{-/-}$ mouse tissues with antibodies to Rassf2; *, non-specific band. (**C**) Survival curve of wild-type, heterozygous, and *Rassf2*$^{-/-}$ mice. Data are for 32 mice of each genotype.

Supplementary Figure S2. Histological analyses and impairments of hematopoietic compartments in *Rassf2*-deficient mice. (**A**) Histological analysis (H&E staining) of thymus, spleen, BM, and liver from wild-type and *Rassf2*$^{-/-}$ mice at 3 weeks of age. (**B**) Total cell numbers for thymus, spleen, and bone marrow (BM) (from both femurs and both tibiae) as well as the number of peripheral blood leukocytes for 3- to 4-week-old *Rassf2*$^{-/-}$ mice and wild-type littermates. Data are means ± SEMs (n = 3 to 5, *P < 0.01). (**C**) Numbers of myeloid (Gr1+CD11b+ and Gr1-CD11b+), B- (B220+IgM- and B220+IgM+), and T- (CD4+ and CD8+) cells in the BM and spleen of 3 week-old wild-type and *Rassf2*$^{-/-}$ mice. Data are means ± SEMs (n = 5, *P < 0.01). (**D**) Relative organ weights for thymus, spleen, and liver to body weight from 4-week-old *Rassf2*$^{-/-}$ mice

and wild-type littermates. Data are means ± SDs (n = 5, *P < 0.01). (**E**) BM cells (1×10^4) from 3-week-old wild-type or *Rassf2*$^{-/-}$ mice were plated in triplicate in cytokine-supplemented methylcellulose medium (Stem Cell Tech) and cultured for 10 days, after which the number of colonies was determined. Representative plates are shown on the left. Quantitative data on the right are means ± SEMs (n = 3, $^{\#}$P < 0.05).

Supplementary Figure S3. Hematopoietic subpopulations after competitive BM transplantation. Competitive BM transplantation was performed as described in the legend to Figure 1E. The percentage contributions of CD45.2$^+$ T- and B cells, and myeloid cells, to donor-derived cells in the BM or peripheral blood (PB), were determined by flow cytometry 8 weeks after transplantation. Data are means ± SEMs (n = 4).

Supplementary Figure S4. Assay for osteoblastic colony-forming units (CFU-OB) in cultures of bone marrow cells. CFU-OBs in BM preparations were determined as described previously, with some modifications (Bellows *et al.*, 1991; Weinstein *et al.*, 1998). Briefly, BM cells (7.5×10^6 cells/well in six-well plates) were cultured for 17 days in α-MEM medium supplemented with β-glycerophosphate (10 mM) and ascorbic acid (50 μg/ml) (Sigma), with a change to fresh medium every 3 days. After fixation with 10% formaldehyde and permeabilization with a 1:1 mixture of acetone and ethanol, colonies were visualized using alkaline phosphatase (ALP) staining. Data are means ± SEMs (n = 5).

Supplementary Figure S5. Effects of *Rassf2* deficiency on the expression of genes

relevant in terms of osteoblast differentiation. At day 6 after osteoblast differentiation commenced, the levels of mRNAs encoding osteoblastogenic proteins (*Runx2*, osterix [encoded by *Sp7*]; osteocalcin [encoded by *Bglap1*]; *Rankl*; M-CSF [encoded by *Csf1*]; and bone sialoprotein [encoded by *Spp1*]) were determined by real-time PCR using the TaqMan® array (Applied Biosystems).

Supplementary Figure S6. Effects of *Rassf2* deficiency on the expression of relevant genes to osteoclasts differentiation. (**A**) Global gene expression profiling analyses in wild-type and *Rassf2*$^{-/-}$ osteoclasts. Expression of marker genes in osteoclast differentiation was analyzed from *Rassf2*$^{-/-}$ BMMs both before (day 0, OCD0) and during their differentiation into osteoclasts (day 3, OCD3) compared with wild-type cells. Data are expressed relative to the values for wild-type cells. (**B**, **C**) RT-PCR analysis of the expression of osteoclast differentiation marker genes and *Rassf2* (**B**) as well as immunoblot analysis of osteoclast differentiation marker proteins (**C**) during osteoclastogenesis from BMMs isolated from *Rassf2*$^{-/-}$ and wild-type mice in the presence of RANKL and M-CSF. The glyceraldehyde-3-phosphate dehydrogenase gene (*Gapdh*) and β-Actin were used for control of RT-PCR analysis and immunoblot analysis, respectively.

Supplementary Figure S7. Enhanced NF-κB signaling in *Rassf2*-deficient osteoclasts and osteoblasts against differentiation stimuli. BMMs (**A**) and osteoblast precursors (**B**) from wild-type and *Rassf2*$^{-/-}$ mice were cultured in the presence of RANKL and M-CSF (**A**) or in osteogenic medium (**B**) for the indicated times. Cell lysates were then subjected to immunoblot analysis with indicated antibodies.

Supplementary Figure S8. Differentially expressed gene (DEG) analysis of putative NF-κB target genes. Putative NF-κB target genes were analyzed for assessing differential expression in *Rassf2*$^{-/-}$ osteoblast precursors or BMMs during differentiation into osteoblasts or osteoclasts (day 7 or day 3; OBD7 or OCD3). Data are expressed relative to the values for wild-type cells. The list of putative NF-κB-dependent target genes is based on data of the previous report (Pahl, 1999).

Supplementary Figure S9. Restoration of osteoclastogenic and osteoblastogenic marker gene expression upon Rassf2 overexpression. After introduction of Rassf2 into *Rassf2*$^{-/-}$BMMs and osteoblast precursors, osteoclast differentiation marker genes (TRAP [encoded by *Acp5*] and *Nfatc1*) and osteoblast marker genes (*Runx2*; osterix [encoded by *Sp7*]; osteocalcin [encoded by *Bglap1*]; bone sialoprotein [encoded by *Spp1*]; *Rankl*; and M-CSF [encoded by *Csf1*]) were analyzed by real-time PCR using the TaqMan® array (Applied Biosystems) at the indicated times.

Supplementary Figure S10. Restoration of osteoclastogenic and osteoblastic marker genes by IKK-DN introduction. After introduction of IKK-DN into *Rassf2*$^{-/-}$ BMMs and osteoblast precursors, osteoclast differentiation marker genes (TRAP [encoded by *Acp5*] and *Nfatc1*) and osteoblast marker genes (*Runx2*; osterix [encoded by *Sp7*]; osteocalcin [encoded by *Bglap1*]; bone sialoprotein [encoded by *Spp1*]; *Rankl*; and M-CSF [encoded by *Csf1*]) were analyzed by real-time PCR using the TaqMan® array (Applied Biosystems) at the indicated times.

Supplementary Figure S11. Expression of Hippo components in the course of osteoclast and osteoblast differentiation. BMMs (**A**) and osteoblast precursors (**B**) from wild-type and *Rassf2*$^{-/-}$ mice were cultured in the presence of RANKL and M-CSF (**A**) or osteogenic medium (**B**) for the indicated times to induce differentiation. Cell lysates were next subjected to immunoblot analysis using the indicated antibodies.

*N.D., not detected.

Supplementary References

Bellows CG, Aubin JE, Heersche JN (1991) Initiation and progression of mineralization of bone nodules formed in vitro: the role of alkaline phosphatase and organic phosphate. *Bone Miner* **14:** 27-40

Pahl HL (1999) Activators and target genes of Rel/NF-kappaB transcription factors. *Oncogene* **18:** 6853-6866

Weinstein RS, Jilka RL, Parfitt AM, Manolagas SC (1998) Inhibition of osteoblastogenesis and promotion of apoptosis of osteoblasts and osteocytes by glucocorticoids. Potential mechanisms of their deleterious effects on bone. *J Clin Invest* **102:** 274-282

Supplementary Figure S1

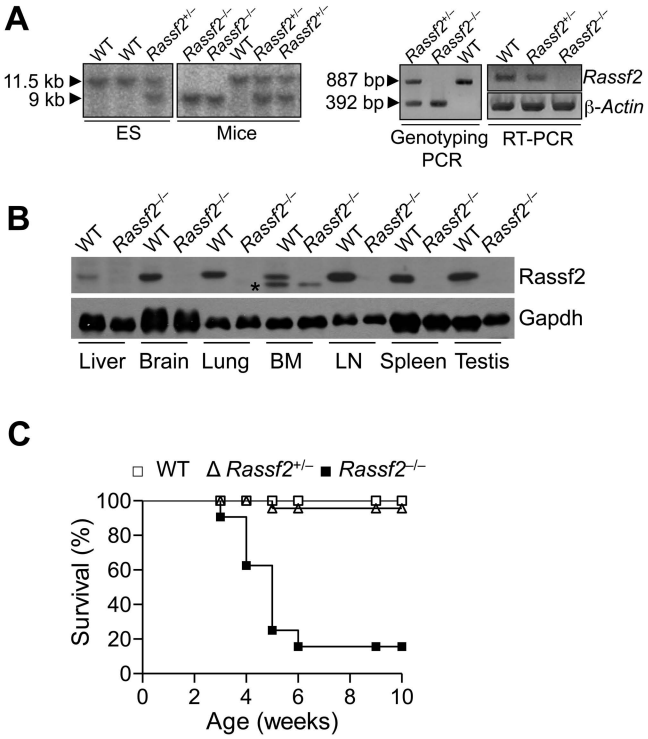

Supplementary Figure S2

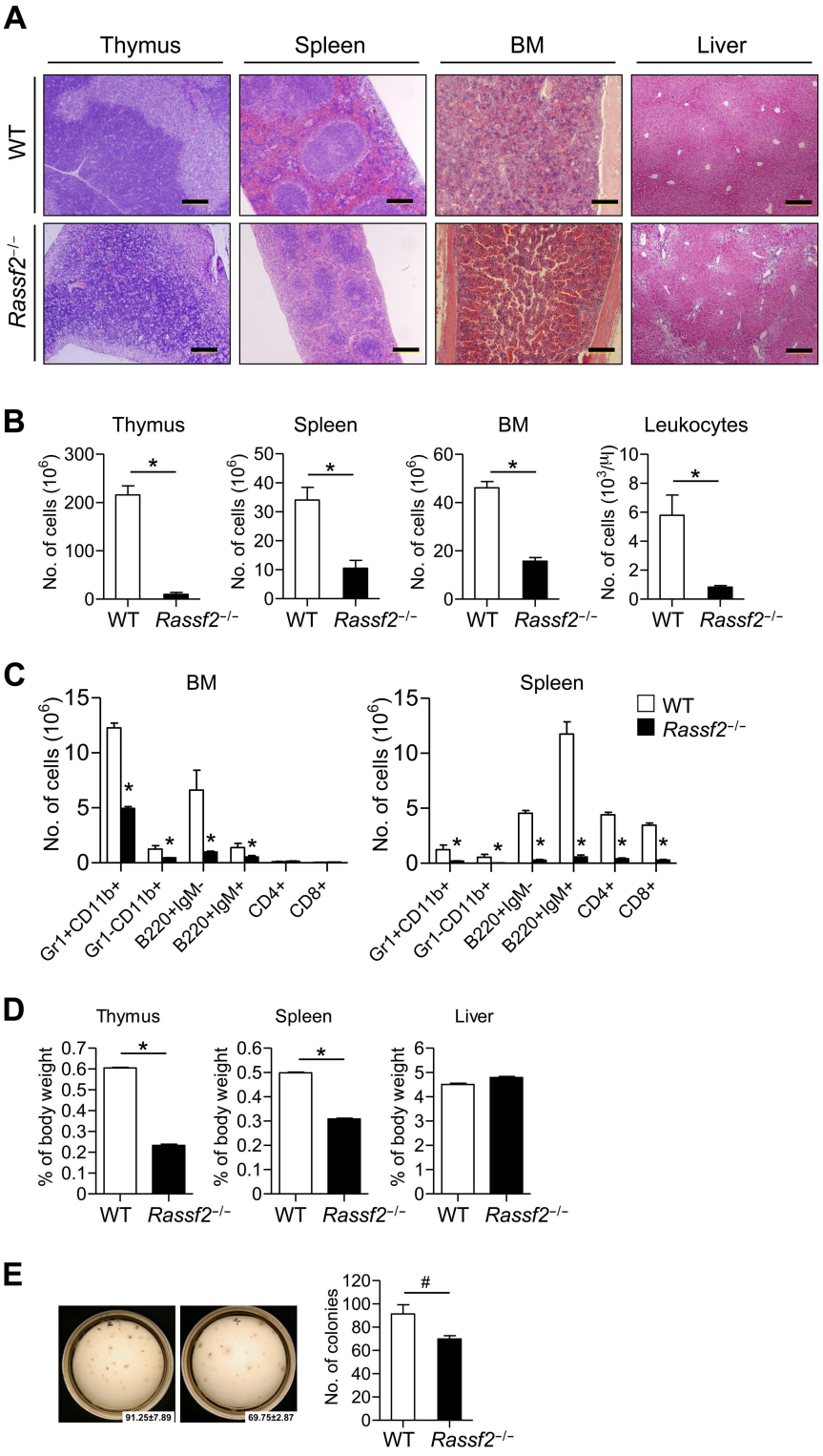

Supplementary Figure S3

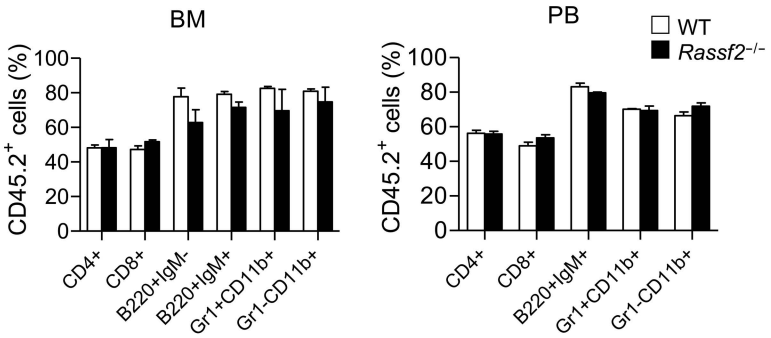

Supplementary Figure S4

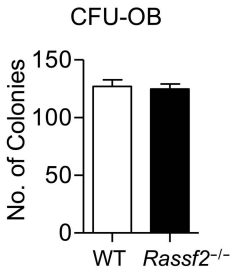

Supplementary Figure S5

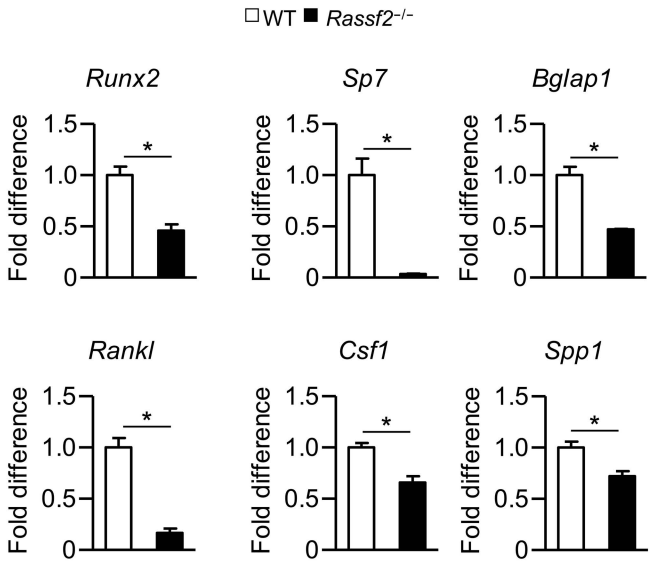

Supplementary Figure S6

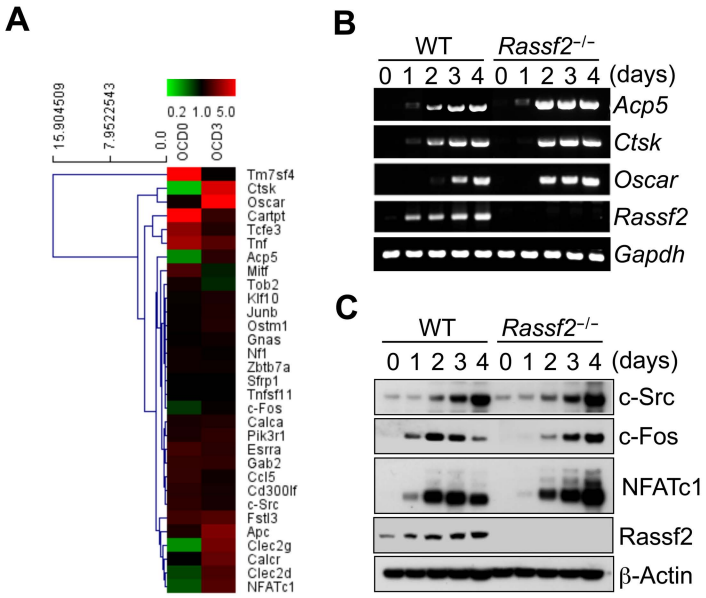

Supplementary Figure S7

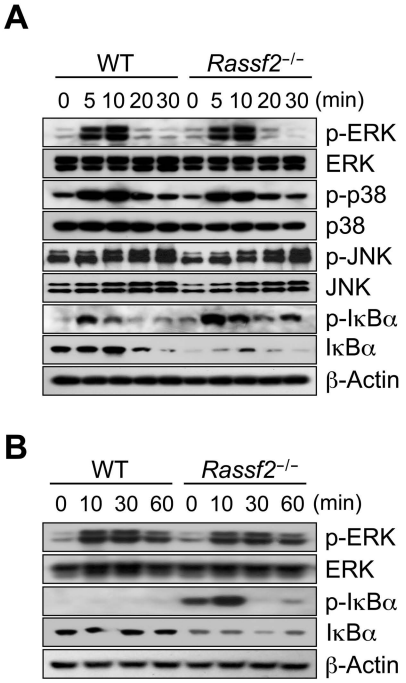

Supplementary Figure S8

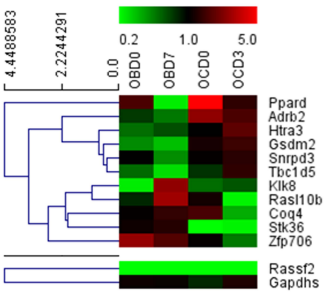

Supplementary Figure S9

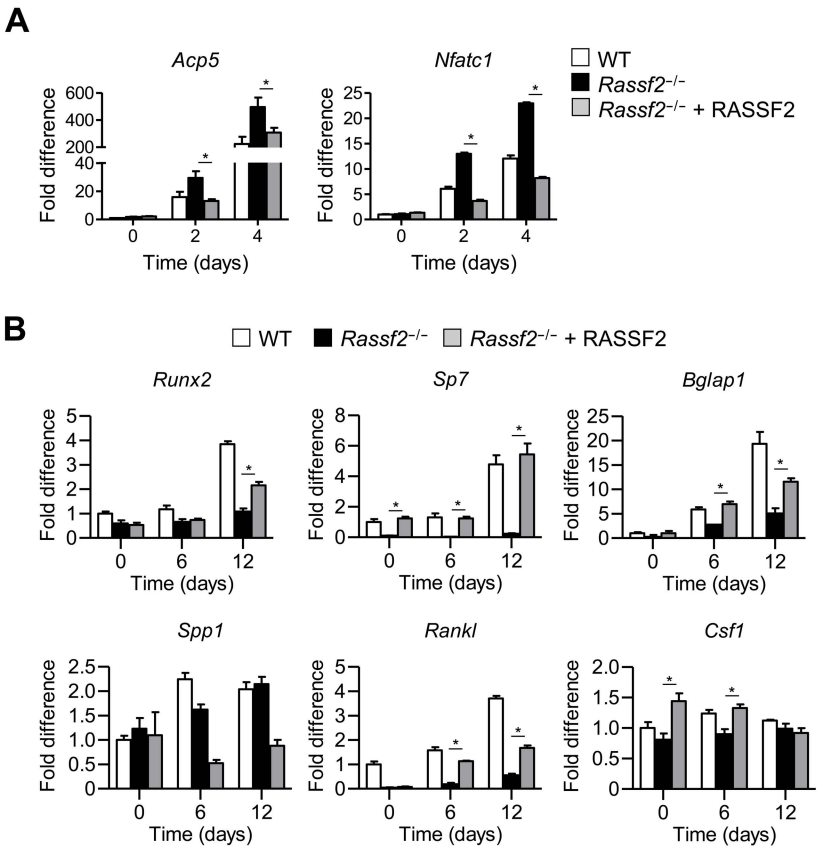

Supplementary Figure S10

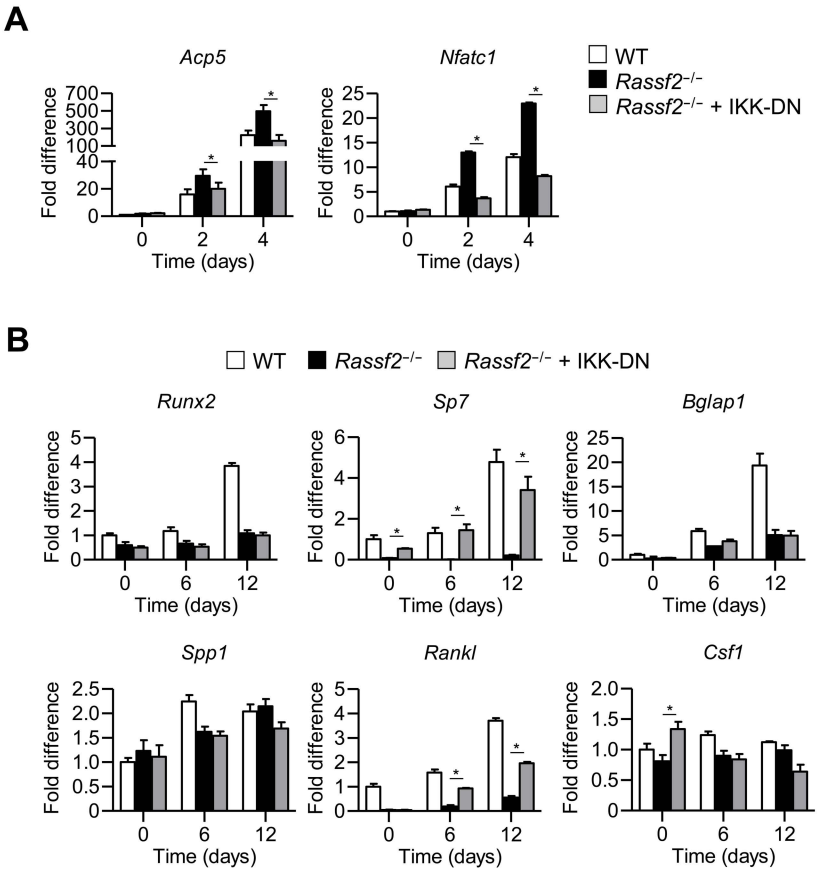

Supplementary Figure S11